

ІНСТИТУТ
ФІЗИКИ
КОНДЕНСОВАНИХ
СИСТЕМ

ICMP-01-17E

T.Patsahan, M.Holovko, A.Trokhymchuk

Computer simulations of the dynamical properties of methane in a
model silica gel

УДК: 538.931; 539.217

РАС: 02.70.Ns, 45.20.Dd, 51.20.+d, 61.43.Gt

Комп'ютерне моделювання властивостей метану у модельному силікагелі

Т.М.Пацаган, М.Ф.Головко, А.Д.Трохимчук

Анотація. Було здійснено комп'ютерне моделювання методом молекулярної динаміки (МД) для Ленарда-Джонсівського флюїда, адсорбованого в модельному силікагелі. Обчислено функції середньоквадратичного відхилення координат та автокореляційні функції швидкостей частинок флюїда при відповідних їх густинах. Отримані результати дали змогу провести кількісний аналіз впливу пористого середовища на динамічні властивості флюїдних частинок, поррахувати коефіцієнти самодифузії при різних параметрах.

Computer simulations of the dynamical properties of methane in a model silica gel

T.Patsahan, M.Holovko, A.Trokhymchuk

Abstract. Molecular dynamics (MD) simulations are performed for a Lennard-Jones fluid adsorbed in a model silica gel to study the individual particle motions. The mean-square displacement and velocity autocorrelation functions of fluid particles are calculated from the MD simulations at densities corresponded to the gas and liquid phases and for different temperatures, and used to analyze their self-diffusion coefficients. It is shown that the presence of porous media reduces the mobility of fluid particles and hence decreases the self-diffusion coefficient.

Подається в Journal of Chemical Physics
Submitted to Journal of Chemical Physics

1. Introduction

The knowledge of the properties of the sorbed fluids in a specific porous solids continue to be of great interest for basic and applied science. Extensive application of porous materials in the petroleum and chemical process industries as catalysts and adsorbents is a powerful stimulus for statistical-mechanical studies. Much theoretical work has been done during the last two decades to model and investigate the physical adsorption in porous media. Primarily this has been concerned with highly idealized pore spaces [geometries] like slit, cylindrical and spherical pores, some specific zeolitic structures and effects of pore shape and size, microscopic structure of pore surface upon thermodynamic, structural, and kinetic properties were extensively investigated. Recently, the models for more complex porous microstructures which characterize gels and Vycor glasses have been developed. These models are aimed to count the influence of macroscopic structure and topology of the pore space upon fluid behavior in porous materials.

There are two major properties of porous materials which affect the measurements of self diffusion. They are related to the extent to which pores are dead ended and tortuous [geometry] and to the degree that the diffusing molecules are adsorbed on surface sites [chemistry]. A relatively simple but nontrivial model for simple-like fluids adsorbed in heterogeneous porous solid have been formulated by Kaminsky and Monson (KM)[7]. This model principally differs from the previously studied[4,5] models for the adsorption of a hard-sphere-like fluids in hard-sphere matrices. The attractive fluid-matrix and fluid-fluid interactions are included in the KM model. Due to this, the effect of temperature on the properties of adsorbed fluid is presented. The fluid-matrix attraction is significantly stronger compared with the fluid-fluid interaction. In addition, this model also is characterized by a quite large asymmetry of diameters of matrix obstacles and of adsorbate fluid atoms. To illustrate the utility of the model, an application to represent the Henry's law constant for methane adsorbed in a silica gel has been used. However, the authors emphasized that a fit of the Henry's constant provides some support but still is far from sufficient for the general conclusion about applicability of the model.

The theoretical tools to investigate these systems include the integral equation theory approaches[2-4] and computer simulation techniques[5-9]. The main attention in the theoretical studies has been paid to the structure and thermodynamical properties. However, little attention has been given to fluid dynamics in heterogeneous microstructures. The

asymmetry of energies and diameters may result in a strong accumulation of the fluid particles in the vicinity of a matrix obstacles. This has been confirmed already by Monte Carlo (MC) computer simulations [7,8]. Thus, we can expect that mobility of fluid particles also could be affected.

In this communication our main goal is to investigate how the dynamical properties of the LJ-like fluid are altered under heterogeneous porous solid confinement. With this aim we apply molecular dynamics (MD) simulation technique to study the behavior of guest simple-like fluid in silica gel. MD simulations are a versatile tool for a detail description of the time evolution of the simulated system, giving access to both structural and dynamic properties. In this paper we study molecular diffusion in a porous medium trying to distinguish between the geometrical and the chemical contributions. The remainder of the paper is organized as follows. The next section describes the potentials of the fluid-fluid and fluid-matrix interactions and the method used for the simulations. The results and discussion are presented in section 3.

2. Modelling and computer simulations

2.1. Model description

The behavior of simple fluids adsorbed in porous medium has been studied by means of a canonical molecular dynamics simulations. The bulk fluid is characterized by the reduced number density, $\rho = N_f \sigma^3 / V$, and is modelled by truncated and shifted 12-6 Lennard-Jones (LJ) potential,

$$u_{ff}(r) = \begin{cases} \phi_{LJ}(r) - \phi_{LJ}(R_f), & r < R_f \\ 0, & r > R_f \end{cases}, \quad (2.1)$$

$$\phi_{LJ}(r) = 4\epsilon \left[\left(\frac{\sigma}{r} \right)^{12} - \left(\frac{\sigma}{r} \right)^6 \right], \quad (2.2)$$

with the parameters: $\epsilon/k = 148.2K$, $\sigma = 0.3817\text{nm}$ that correspond to methane-methane interaction. All length scales are expressed in units of σ .

The model for porous adsorbent is reduced to an equilibrium configuration of N_m hard spheres [obstacles] of the diameter D . The ratio of the volume occupied by hard-core obstacles to the volume, V , of the whole sample is $\phi = (\pi/6)N_m D^3 / V$ and defines the adsorbent porosity, $1 - \phi$. It already has been shown that this is a reasonable first approximation to the structure of silica gel [6].

The essence of the simulations of pore fluid is the modelling of the interaction between fluid molecules [admolecules] and the silica spheres. In this case it is important how we specify a fluid-surface interaction, i.e. an interaction between a fluid particle and the spherical surface of a matrix particle. The system we simulated was based on the model developed by Kaminsky and Monson (KM) [7] for methane adsorbed in a microporous silica gel. The truncated and shifted fluid-surface interaction in the frame of this model has the form:

$$u_{fm}(r) = \begin{cases} \infty, & r < \frac{1}{2}D \\ \phi_{KM}(r) - \phi_{KM}(R_m), & \frac{1}{2}D < r < R_m \\ 0, & r > R_m \end{cases}, \quad (2.3)$$

where [7,8]

$$\phi_{KM}(r) = \frac{2}{3}\pi\rho_s D^3 \epsilon_s \left[\frac{(r^6 + 21/20D^2r^4 + 3/16D^4r^2 + D^6/192)d^{12}}{(r^2 - D^2/4)^9} - \frac{d^6}{(r^2 - D^2/4)^3} \right]. \quad (2.4)$$

For convenience of the reader we list the set of parameters of the potential functions: $d = 0.33\text{nm}$, $\rho_s = 44\text{nm}^{-3}$, $\epsilon_s/k = 339K$ and $D = 7.055\sigma$.

Besides that we introduce a potential of the repulsive (non-attractive) interaction between the fluid and matrix particles

$$u_{fm}^{REP}(r) = \begin{cases} u_{fm}(r), & r < R_0 \\ 0, & r > R_0 \end{cases}, \quad (2.5)$$

where $R_0 = 4.1526\sigma$ was chosen in the way $u_{fm}(R_0) = 0.0$ to be equal to zero.

The potential functions for the fluid-fluid and fluid-surface interactions both have been spherically truncated with cut-off radii, R_f and R_m , respectively. To eliminate the impulsive contribution from the discontinuity of the potentials at cut-off distance to the force, both, $u_{ff}(r)$ and $u_{fm}(r)$, have been shifted on the magnitude of the interaction energy at cut-off distance. Particularly, we used $R_f = 2.56\sigma$ for adsorbed fluid, and $R_m = 12\sigma$ for fluid-surface interactions.

The properties of fluid in porous solid environment are determined by the interaction within fluid particles, and interaction of fluid particles

with the static obstacles. The nature of latter is specific, i.e. includes into the modelling the chemical nature of the gel and is a dominant factor upon fluid behavior in porous medium. However, often the role of fluid-obstacle interaction is approximated and reduced to the effects such as geometrical obstructions, hydrodynamic drag, etc. To shed more light on the role of fluid-solid obstacle interaction and reveal the impact of geometrical and chemical effects on the behavior of pore fluid, four different systems have been simulated. The system A corresponds to the pure or bulk fluid, i.e. N_f fluid particles in a volume V . The system B and C consist of the same fluid but infused into porous solid with attractive [$u_{fm}(r)$ interaction potential] and repulsive [$u_{fm}^{REP}(r)$ interaction potential] pore surfaces, respectively. The system D was also bulk fluid, like in system A, but in the volume, $V' = V(1 - \phi)$, which corresponds to the free volume in porous solid in the systems B and C.

2.2. Molecular dynamics simulations

The canonical ensemble molecular dynamics (MD) simulations were conducted adopting the commonly used [classical] Verlet velocity algorithm. The introduced modification was caused by the presence in simulation system of the two quite distinct component, i.e. adsorbed fluid and adsorbent medium. Concerning the to this, we are dealing with the system of the large static spherical obstacles and of the mobile fluid particles of atomic size [tracer]. Thereby, we should solve the equations of motion exclusively for the fluid particles, similarly to the case of the bulk simple fluid system, but with the obstacles taken into account. The used algorithm is not time consuming and is quite efficient. Care has to be taken with respect of the total momentum which could not be equal zero. We monitored the total momentum of the system as a function of time and our conclusion is that it has the negligible fluctuations around zero value and does not influence the generated simulation data.

All fluid-matrix simulations reported in the present study have been carried out for the fixed number of matrix particles, [$N_M = 32$], which have been set randomly in the cubic box with basic size, $L = V^{1/3}$. This size is determined by the volume fraction of matrix particles which was fixed at the value corresponded to the KM model, $\phi = 0.386$, i.e. the porosity of the matrix, $1 - \phi$, was maintained constant throughout. The initial configurations of the fluid particles were set randomly in each simulation run and their number, N_f , has been depended on the considered fluid density and the range of N_f values was 585 – 5385. For each set of the parameters of adsorbed fluid, i.e. temperature and density, we realized five different configurations of the matrix particles. The final

results, which are reported, have been obtained by the averaging over these configurations. Except cases are specified additionally the displayed values of results in the paper is presented in dimensionless units due to the common normalization. To monitor the influence of the confinement on the fluid behavior, we also performed the canonical MD simulations for the fluid particles only.

3. Results and discussion

We performed MD simulations for two fluid densities, $\rho_f = 0.0384$ and 0.3534 which can be associated with the density of the gas and liquid phases of LJ-like fluid. To choose the temperature region, we exploit the fact that in practice the adsorption in silica gels usually is performed at supercritical temperatures with respect to the bulk fluid. To ensure the single phase conditions, the reduce temperature, $T^* = kT/\epsilon$, has been varied within the range from $T^* = 1.2$ till $T^* = 2.0$, which is above the bulk gas/liquid critical temperature [$T_c^* \sim 1.1$] for the current fluid model [12]. Hence, such temperature range will be the supercritical for the fluid adsorbed in porous medium as well [13].

3.1. Radial distribution functions

We proceed with the discussion of the fluid-fluid, $g_{FF}(r)$, and fluid-surface, $g_{FM}(r)$, radial distribution functions (RDFs). There were a few reasons that we persecuted calculating RDFs. We already mentioned one of them, i.e. to verify the MD algorithm employed in the present study through the comparison obtained MD data against those computed by Vega et al. [8] from GCMC simulations. The second reason was to get conclusions about the influence of the porous environment on the fluid-fluid RDF through the comparison with the bulk data at the same temperature and density conditions. The next, we were curious about the local ordering of fluid particles inside of porous solid which could be obtained from the fluid-surface RDF [or fluid density profiles]. Finally, we were aimed to involve the results on the structure ordering of the atoms of adsorbed fluid into the interpretation of their dynamical properties.

The main results are summarized on Figs. 1-3. The data are presented for two reduced temperatures, $T^* = 1.2$ and 2 , which correspond to the low and upper boundaries of the temperature range where dynamical properties have been studied and discussed. This makes possible to reveal the effect of the temperature on the structural properties of the gas-like and liquid-like adsorbates.

First of all, in all cases available [Figs. 1 and 2] we found excellent agreement between canonical ensemble MD data and those obtained from grand canonical ensemble MC simulations of Vega et al. [8]. Small discrepancies should be attributed to the details of potential truncation.

Analyzing the fluid-pore RDFs for attractive pore [Figs. 1 and 2], we observe the layered structure of fluid particles with well-defined contact layer around silica spheres at both densities of adsorbate. At fixed density, the peaks height of fluid-pore RDFs increase with lowering temperature as expected. However, at fixed temperature, the same peaks height decrease with increasing density of pore fluid, i.e. going from gas-like to liquid-like adsorbate. Opposite trends occur in repulsive pore solids [Fig. 3] with fluid-surface interaction potential Eq. 2.5, where the value of fluid-pore contact increases with increasing density, as expected. No layering is observed for a gas-like adsorbate for repulsive pore.

Using the fluid-silica radial distribution functions one can estimate average numbers of fluid particles in a contact layer. To do this, we calculated the running coordination number function,

$$n(r) = 4\pi\rho \int_0^r g_{fm}(x)x^2 dx , \quad (3.6)$$

for the fluid particles adsorbed on the solid obstacles. We can define the first coordination number, n_1 , as the value of $n(r)$ at the distance r corresponded to the position of the first minima of the fluid-matrix radial distribution function, $g_{fm}(r)$. These data are collected in Table 1. One can see that the number of fluid particles surrounding a matrix particles increases with increasing of the fluid density. First coordination number has a very small dependence from temperature for higher density.

3.2. Dynamical properties

The main subjects of our interest from the point of view of dynamic [diffusion] properties were two dynamic functions. The first is the time evolution of the self-part of mean square displacement (MSD), as defined by

$$\langle r^2(t) \rangle = \frac{1}{N_f} \left\langle \sum_i |\mathbf{r}_i(t) - \mathbf{r}_i(0)|^2 \right\rangle , \quad (3.7)$$

where the $\mathbf{r}_i(t)$ are the space coordinates of the center of mass of fluid particles at time t . The second dynamic functions which we evaluated during simulation runs was the self-part of the normalized velocity autocorrelation function (VACF),

$$\psi(t) = \frac{\sum_i \langle \mathbf{v}_i(t) \mathbf{v}_i(0) \rangle}{\sum_i \langle \mathbf{v}_i(0) \mathbf{v}_i(0) \rangle}, \quad (3.8)$$

with $\mathbf{v}_i(t)$ being the individual velocity of fluid particles at time t . The average $\langle \dots \rangle$ is within the canonical ensemble and along the whole trajectory of each particles, i.e. $t_0 \geq t \geq t_0 + t_{max}$ [$t_0 \sim 440$ ps]. The trajectory information can be employed to compute the time dependent diffusivity, $D(t)$. This can be evaluated either with the help of Green-Kubo expression,

$$D(t) = \frac{1}{3} \int_0^t \psi(t') dt', \quad (3.9)$$

or by using the Einstein relation,

$$D(t) = \frac{1}{6} \frac{\partial \langle r^2(t) \rangle}{\partial t}. \quad (3.10)$$

The total length of the trajectory, t_{max} , was different for a gas-like and liquid-like fluids as well as different for a bulk and pore fluids. Longer trajectories were needed in order to achieve a good statistical description of the MSD [diffusive process] at low density. At the fixed density, final trajectories which correspond to the macroscopic self-diffusion coefficient D are shorter when the fluid is adsorbed in porous medium. Relatively shorter trajectories [comparatively to MSD] are needed for recording VACF to ensure their decay to a final value of zero [within statistical accuracy of the simulation data]. The random microstructure of silica gel may leads, in general, to the anisotropy of the diffusion process. However, we were interested in the total [average] features of the particle dynamics only.

The mean square displacements as a function of the observation time for low and high densities of adsorbed fluid are given in Figs. 4a and 4b, respectively. Each figure contains two groups of curves which correspond to free [bulk] fluid [dashed lines] and fluid infused into porous media [solid lines] under the same density and temperature conditions. As it was known from the bulk studies, the particles have much bigger displacement for low fluid density than for high fluid density. The displacement also is bigger at higher temperature than at lower temperature. The presence of the silica spheres leads to the slowing down of the diffusion motion. Fluid particles diffuse significantly longer distances in the bulk fluid in the case of both densities and for all studied temperatures.

The time dependence of the mean square displacement is different at different periods of time. Three time regimes has been distinguished

[16,17] by analyzing the movement of the tracer from the time dependence of the correlation function of the scattered-light intensity: (i) the diffusion process is normal at short times, (ii) becomes to anomalous at moderate times and (iii) returns to be normal for large delay times. Normal diffusion assumes here that time dependence of the fluid particle dynamics are subject to the law of deterministic motion [Newtonian dynamics] on the initial ballistic phase and satisfy the Fick's second law and isotropy [Euclidean dynamics] on a long time scale. In order to extract more information from the simulation data, log-log plots of MSD turn out to be very helpful [14,15]. This is shown in Figs. 4c and 4d for the low and high density, respectively. Two linear regions [at the initial and final stage] easily can be recognized for each set of the data presented on these plots. In general, every linear region on logarithmic scale indicates a distinct diffusive regime, described by a power law behavior $D(t) \sim t^\alpha$ where the power α can be determined from the slope of the straight line fitting the data. Below $t^* \sim 1$, the straight line has slope $\alpha = 2$, corresponding to Newtonian dynamics, i.e. $\langle r^2(t) \rangle = v^2(0)t^2$. Well above $t^* \sim 1$, the straight line has slope $\alpha = 1$ corresponding to Einsteinian regime, i.e. $\langle r^2(t) \rangle = Dt$. In the case of a bulk fluid these two straight lines intersect, defining the characteristic distance λ and time τ that separate the two diffusive regimes. Between these two regimes, the displacement profile is not linear, representing the transition from deterministic [quasifree] particle motion to the Einsteinian diffusion [particle motion is affected by the collisions with the other particles]. Comparing the bulk MSD curves with the simulation data for the MSD in a gas-like adsorbate [Fig. 4c] we see that, indeed, as it was found experimentally in studies of probe diffusion through polyacrylamide gels [16], the shape of the MSD profile has additional linear region in between two normal diffusion regimes. The slope of this linear region for low density adsorbate is about $\alpha = \frac{3}{2}$ indicating a perturbation of the particle trajectory due to collision with obstacles. This behavior only quantitatively depend on the nature of the surface [attractive or repulsive]. For attractive surface the transition time from ballistic behavior to anomalous diffusion is shorter as well as crossover from anomalous diffusion to the normal diffusion over long distances is more delayed. After entering the anomalous diffusion regime, MSD is permanently larger for repulsive obstacles.

Anomalous diffusion is strongly affected by the density of the guest fluid [Fig. 4d]. In particular, the liner region at moderate times practically does not exist for liquid-like adsorbate, i.e. particles are found to follow normal [Brownian] diffusion directly after an initial ballistic phase. As in the case of low density, time dependence of the MSD is the

same for both attractive and repulsive surfaces. The explanation for this behavior is that at high density of the pore [adsorbed] fluid, the surface coverage of obstacles is very high for both [repulsive and attractive] surfaces [see the first coordination shell numbers] and tracer cannot "see" the pure obstacles but only particles of the adsorbed layer. Due to this, the diffusion process in silica gel at high density of adsorbed fluid qualitatively is similar to the dynamics of higher density [free volume] bulk fluid.

A noticeable difference in the dynamical properties of gas-like and liquid-like pore fluid is evidenced by the data calculated for VACFs which are shown on Fig. 5a. For each density the set of five curves are displayed to illustrate the temperature effect. The two groups of autocorrelation functions relax following the qualitatively different patterns, which means that the motions of the individual particles are essentially different. It is notable that $\psi(t)$ relaxes much more faster in the case of higher density adsorbate and assume the negative values at $t^* \sim 1$. The slow relaxation at low density is superimposed by a weak non periodic oscillating pattern.

The normalized VACFs, evaluated for bulk, free volume, and both attractive and repulsive fluid-surface interactions are shown on Fig. 5b and 5c for gas-like and liquid-like adsorbate, respectively. One can see, that $\psi^*(t)$ of the adsorbed fluid decays faster than that in the bulk fluid, regardless of time. The deviation is started to be observed from the times $t^* \sim 0.2$ and appears to be significant at times greater than the time t_{con}^* roughly required for the molecules to have diffused into contact with silica sphere. In the contrast to the bulk fluid, the well defined minima, in the case of matrix fluid, is seen at short times.

We calculated self-diffusion coefficient of fluid versus time t^* from our VACF and MSD functions and results are displayed on Fig. 6. One can see that the self-diffusion coefficient of matrix fluid has a constant value for large time.

3.3. Macroscopic self-diffusion coefficient

Both of the expressions Eqs. 3.9 and 3.10 can be used to predict the macroscopic diffusion coefficient, but in both cases, $\psi(t)$ and $\langle r^2(t) \rangle$ have to be known at large times [large compared to the characteristic time of correlations between the tagged particle and its immediate neighbors]. At these times, which determine the hydrodynamic region, we can expect that $\langle r^2 \rangle$ behaves as a linear function of t and the self-diffusion coefficient can be calculated as the limiting slope of the MSD. In such context, an evaluation of the self-diffusion coefficient through the veloc-

ity autocorrelation functions is more rigorous. In the bulk case, both procedures give consistent results with a similar uncertainty which is of the order of 5% [11].

The results of our calculations of the macroscopic self-diffusion coefficients by using Eqs. 3.9 and 3.10 are collected in Figs. 7, 8 and 9. Two sets of data for each temperature and density case correspond to the self-diffusion coefficients obtained from MSDs and from VACFs. We see, that in all cases the agreement between both procedures is quite reasonable.

The ratio of the diffusion coefficients of the adsorbed fluid [system B] and bulk fluid of effective density [system D] to the corresponding quantity in bulk region [system A], D_{ads}/D_{bulk} and D_{eff}/D_{bulk} , respectively, show clearly that D_{ads} changes relative to bulk fluid and to fluid with effective [higher] density [Fig. 7]. This means, that diffusion processes are significantly affected by silica gel and are slower in this porous solid. This effect is more pronounced for low adsorbed fluid density where D_{ads} is one order of magnitude lower than for free bulk diffusion [half of order of magnitude for high adsorbed fluid density]. Examining these results, we see that most of the decrease in D_{ads} is caused by the confinement. The substitution of the adsorbed fluid by the bulk fluid with the effective [higher] density that, indeed, is associated with decrease of diffusion, does not correspond and is not equivalent to the effect of confinement. Not only the magnitude of the diffusion coefficient [D_{eff} is always higher than D_{ads} at the same density and temperature] but dependence on temperature and density in both cases are qualitatively different: ratio D_{ads}/D_{bulk} increases with rise of temperature while D_{eff}/D_{bulk} decreases; ratio D_{ads}/D_{bulk} for low density is smaller than for higher density while D_{eff}/D_{bulk} has an opposite trend.

The effect of temperature on the diffusivity can be discussed from Fig. 8. The plot shows that diffusion of gas-like and liquid-like adsorbates in a silica gel is an activated process, i.e. it follows the Arrhenius equation,

$$D = D_0 \exp(-E_a/RT), \quad (3.11)$$

where D_0 is called the preexponential factor, E_a is the activation energy, R is the gas constant, and T is the temperature. The estimate for activation energy is 3.53 kJ/mol for low density particles and 1.80 kJ/mol for particles in a liquid-like phase.

The absolute values of the model predictions for self-diffusion coefficient for methane adsorbed in silica gel are shown on Fig. 9. On this figure we also can see the dependence of the self-diffusion coeffi-

cient on temperature: with rise of the temperature, diffusion becomes faster and is accelerated at low density relative to high density. Our estimates, $D_{ads} = 0.875 \cdot 10^{-7} m^2/s$, for the low density adsorbate at $T = 296K$ are in a reasonable agreement with the experimental value $0.952 \cdot 10^{-7} m^2/s$ for the effective pore diffusivity of the methane gas on silica gel at $T = 310K$ [1].

4. Conclusions

Summarizing, the canonical ensemble MD simulations are used to study the microstructure and dynamics of the simple fluids adsorbed in a porous medium. It follows, that adsorption of the simple fluid into the porous medium results in the formation of the adlayer structure of the fluid particles near the surface of the large matrix particles.

It can be seen clearly that the behavior is dependent on (i) the presence of static obstacles, (ii) the density of adsorbed fluid and (iii) the temperature.

The presence of the matrix particles affect the mobility of fluid particles. The self-diffusion coefficients are less for matrix fluid than for bulk fluid. It is shown, that self-diffusion decreases not only due to the decreasing of the space available for adsorption but mainly due to the geometry of the confinement. At low fluid density self-diffusion strongly depends on the temperature. The effect of temperature decreases when the density of adsorbate increases.

The extent to which dynamical properties of simple-like fluids within the porous silica gel are determined by surface diffusion requires additional studies and will be reported elsewhere.

References

1. Gangwal, S.K; Hadgins, R.R.; Silveston, P.L. *The Canadian J. of Chem. Engineering*, **1979**, *57*, 609.
2. Madden, W. G.; Glandt, E. D. *J. Stat. Phys.* **1988**, *51*, 537.
3. Given, J. A.; Stell, G. *J. Chem. Phys.*, **1992**, *97*, 4573.
4. Fanti, L. A.; Glandt, E. D.; Madden, W. G. *J. Chem. Phys.* **1990**, *93*, 5945.
5. Lomba, E.; Given, J. A.; Stell, G.; Weis, J. J.; Levesque, D. *Phys. Rev. E* **1993**, *48*, 233.
6. MacElroy, J. D.; Raghavan, K. *J. Chem. Phys.* **1990**, *93*, 2068.
7. Kaminsky, R. D.; Monson, P. A. *J. Chem. Phys.* **1991**, *95*, 2936.

8. Vega, C.; Kaminsky, R. D.; Monson, P. A. *J. Chem. Phys.* **1993**, *99*, 3003.
9. Trokhymchuk, A.; Pizio, O; Holovko, M.; Sokolowski, S. *J. Chem. Phys.* **1997**, *106*, 200.
10. Labik, S.; Malijevski, A.; Vonka, P. *Mol. Phys.* **1985**, *56*, 709.
11. Levesque, D.; Verlet, L. *Phys. Rev. A*, **1970**, *2*, 2514.
12. Trokhymchuk, A.; Alejandre, J. *J. Chem. Phys.* **1999**, *111*, 8510.
13. Trokhymchuk, A.; Sokolowski, S. *J. Chem. Phys.* **1998**, *109*, 5044.
14. S. El Amrani and M. Kolb, *J. Chem. Phys.* **98**, 1509 (1993).
15. P. Demontis, G. B. Suffritti, and A. Tilocca, *J. Chem. Phys.* **105**, 5586 (1996).
16. Y. Suzuki and I. Nishio, *Phys. Rev. B*, **45**, 4614, 1992.
17. P. A. Netz and T. Dorfmueller, *J. Chem. Phys.* **103**, 9074 (1995).

Table 1. The number of fluid particles in the contact layer around silica sphere

T^*	ρ	attractive pore		repulsive pore	
		r_{min}	n_1	r_{min}	n_1
1.2	0.0384	4.95	34	5.0	13
	0.3534	4.7	141	4.8	115
2.0	0.0299	5.15	23	-	-
	0.3534	4.75	139	-	-

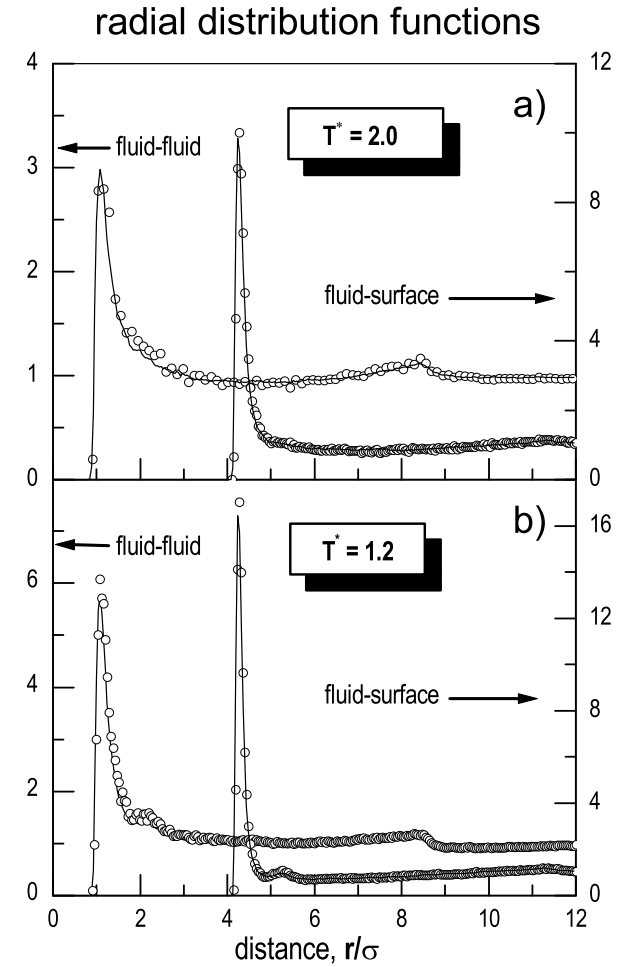


Figure 1. Attractive fluid-matrix interaction. Fluid-fluid and fluid-matrix radial distribution functions, $g_{FF}(r)$ and $g_{FM}(r)$, respectively, for low fluid density at the temperatures $T^* = 2.0$ (part a) and 1.2 (part b). Solid lines correspond to the data obtained from MD simulations of this work, circles - from GCMC simulations of Vega *et al.*[8].

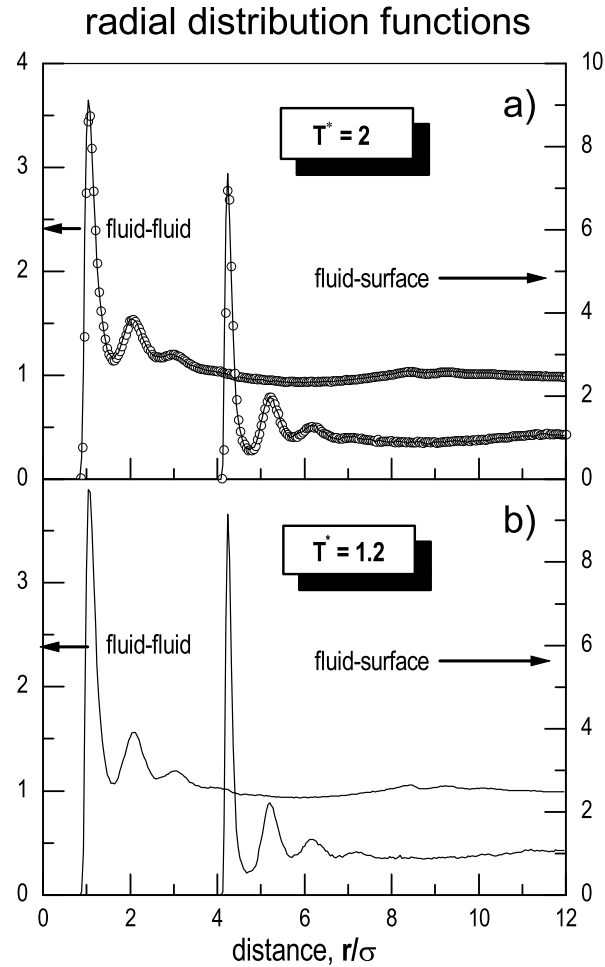


Figure 2. The same as in Fig. 1 but for high fluid density.

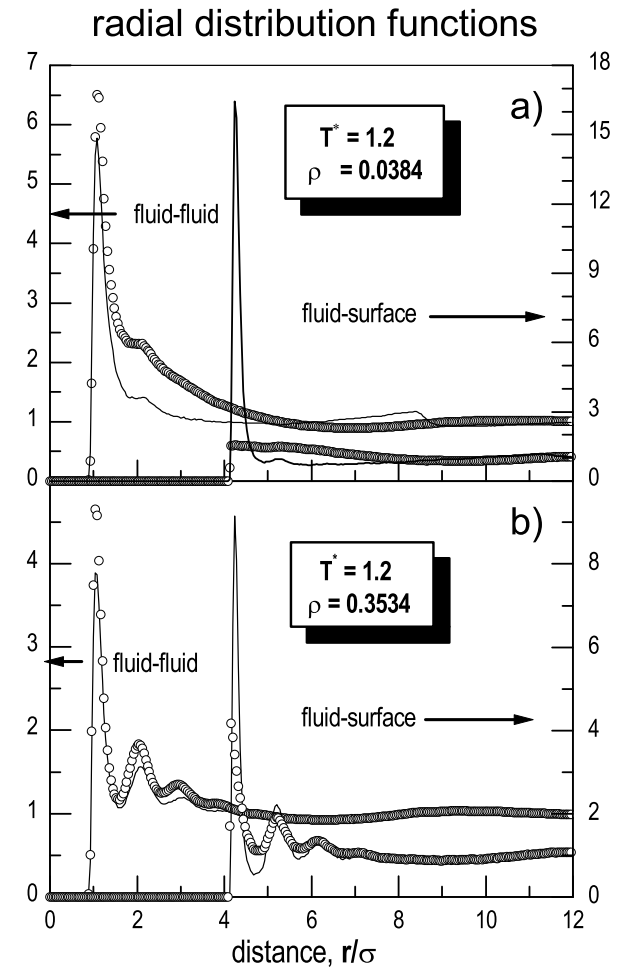


Figure 3. Comparison of the attractive and repulsive fluid-matrix interactions. Fluid-fluid and fluid-matrix radial distribution functions, $g_{FF}(r)$ and $g_{FM}(r)$, at temperature $T^* = 1.2$ for low fluid density $\rho_F^* = 0.0384$ (part a) and high fluid density, 0.3534 (part b). Results are obtained from MD simulations of this work. Solid lines correspond to the data for attractive fluid-surface interaction (KM model), circles - for repulsive fluid-matrix interaction.

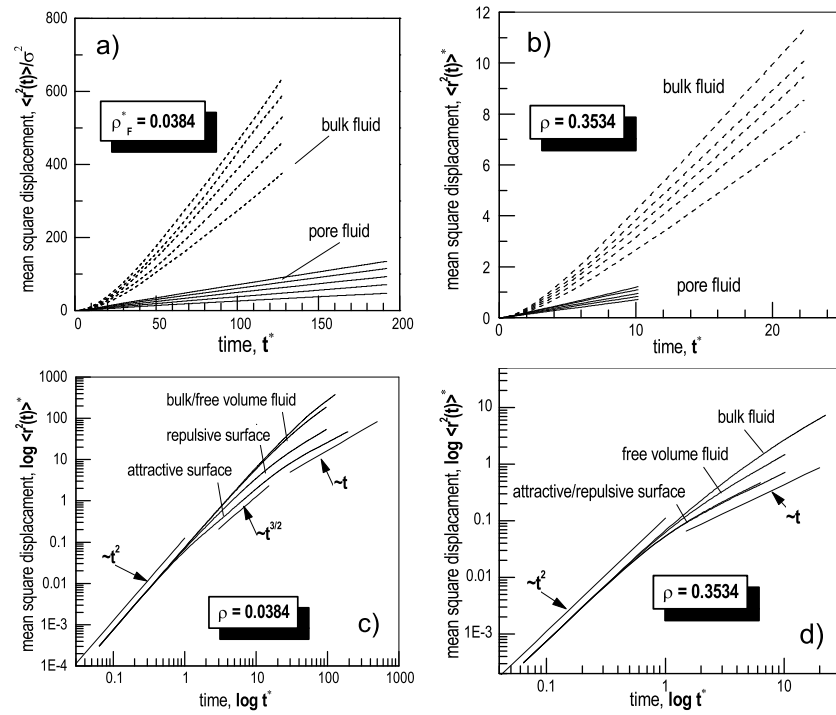


Figure 4. Mean-square displacement, $\langle r^2(t) \rangle$. Part (a): comparison of the bulk and pore fluid at different temperatures for low fluid density, $\rho_F^* = 0.0384$; part (b): comparison of the bulk and pore fluid at different temperatures for high density, $\rho_F^* = 0.3534$; part (c): comparison of the bulk fluid, free volume fluid and pore fluid with an attractive and repulsive fluid-matrix interaction at temperature $T^* = 1.2$ for low density, $\rho_F^* = 0.0384$; part (d): the same as in part (c) but for high fluid density, $\rho_F^* = 0.3534$.

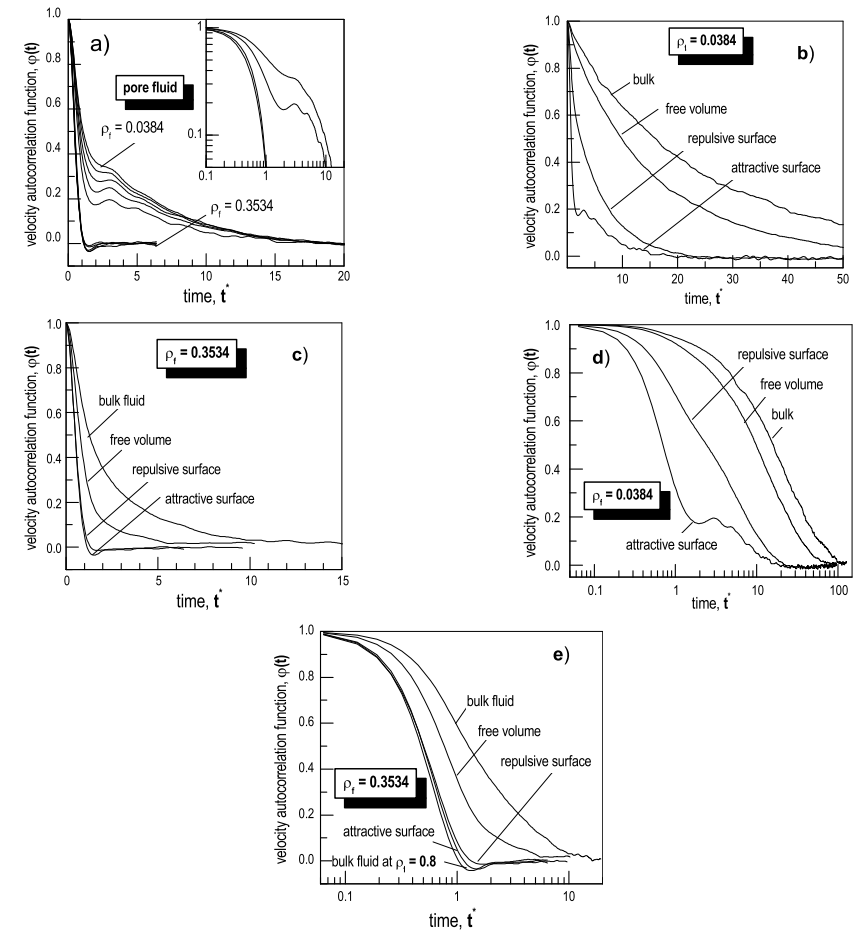


Figure 5. Fluid particles normalized velocity autocorrelation functions $\psi(t)$. Part (a): comparison of pore fluids for low and high densities at different temperatures; part (b): comparison of the bulk fluid, free volume fluid and pore fluid with an attractive and repulsive fluid-matrix interaction at temperature $T^* = 1.2$ for low density, $\rho_F^* = 0.0384$; part (c): the same as in part (c) but for high fluid density, $\rho_F^* = 0.3534$. part (d): the same as in part (b) but in log scale. part (e): the same as in part (c) but in log scale.

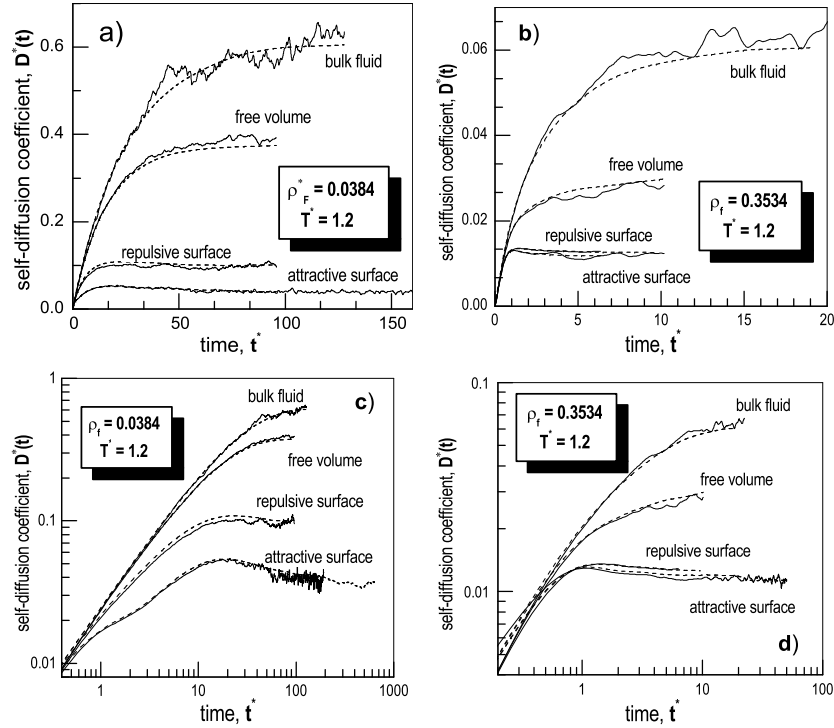


Figure 6. Self-diffusion coefficient of fluid versus time, $D^*(t)$. Solid lines correspond to the results obtained from MSD, while dashed lines correspond to the results evaluated from ACF. Part (a): comparison of the bulk fluid, free volume fluid and pore fluid with an attractive and repulsive fluid-matrix interaction at temperature $T^* = 1.2$ for low density, $\rho_F^* = 0.0384$; part (b): the same as in part (a) but for high fluid density, $\rho_F^* = 0.3534$. part (c): the same as in part (a) but in log scale. part (d): the same as in part (b) but in log scale.

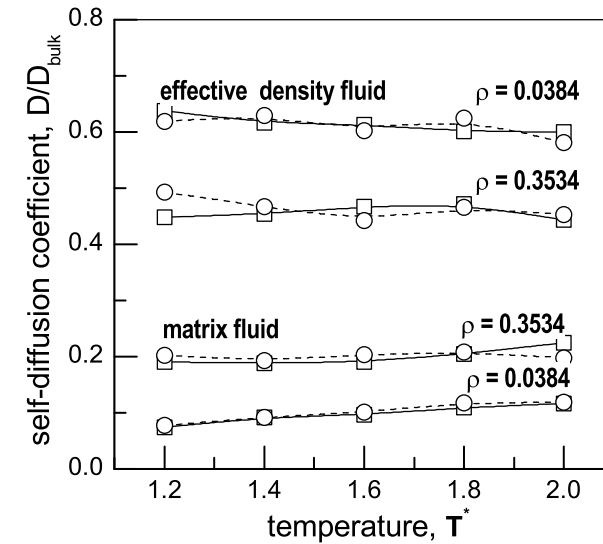


Figure 7. Relative self-diffusion coefficient of the adsorbed fluid $[D_{ads}/D_{bulk}]$ and the bulk fluid in an effective volume $[D_{eff}/D_{bulk}]$ versus temperature T^* , for a low and high fluid densities, $\rho_F^* = 0.0384$ and 0.3534 , respectively. The meaning of solid and dashed lines are the same as in Fig.6.

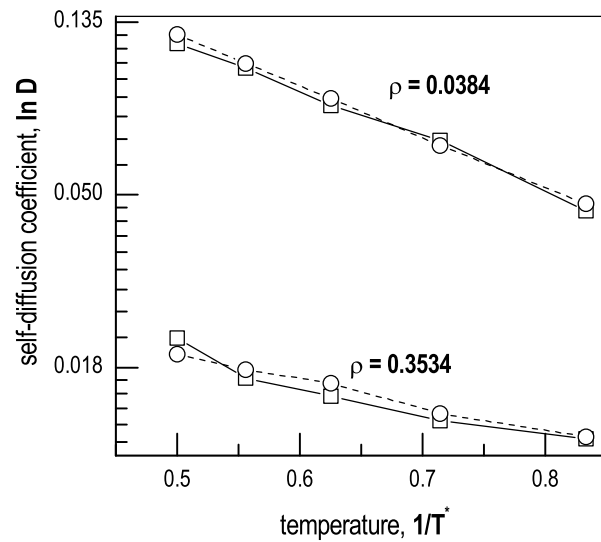


Figure 8. Logarithmic self-diffusion coefficient of adsorbed fluid particles versus $1/T^*$ for a low and high density fluids, $\rho_F^* = 0.0384$ and 0.3534 , respectively. The meaning of solid and dashed lines are the same as in Fig.6.

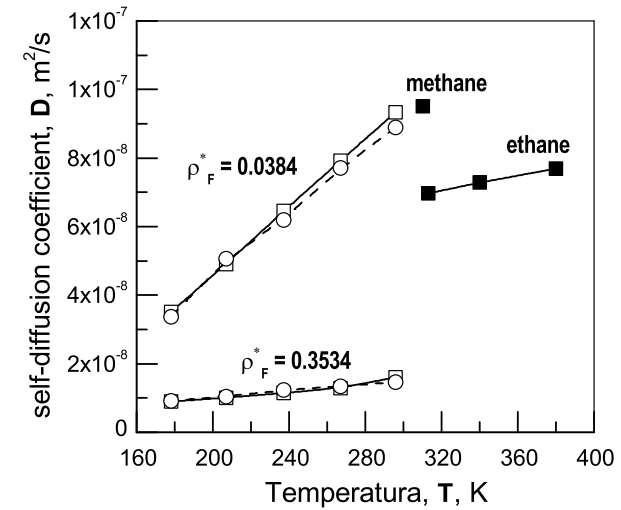


Figure 9. Self-diffusion coefficient of adsorbed the methane particles in the model silica gel versus temperature T in real units for a low and high density fluids, $\rho_F^* = 0.0384$ and 0.3534 , respectively. Square symbols with solid line correspond to the results obtained from MSD, while circles with dashed line correspond to the results evaluated from ACF. Filled symbols corresponds experimental data for methane and ethane in porous media (near conditions).

Препринти Інституту фізики конденсованих систем НАН України розповсюджуються серед наукових та інформаційних установ. Вони також доступні по електронній комп'ютерній мережі на WWW-сервері інституту за адресою <http://www.icmp.lviv.ua/>

The preprints of the Institute for Condensed Matter Physics of the National Academy of Sciences of Ukraine are distributed to scientific and informational institutions. They also are available by computer network from Institute's WWW server (<http://www.icmp.lviv.ua/>)

Тарас Миколайович Пацаган
Мирослав Федорович Головка
Андрій Дмитрович Трохимчук

КОМП'ЮТЕРНЕ МОДЕЛЮВАННЯ ВЛАСТИВОСТЕЙ МЕТАНУ У
МОДЕЛЬНОМУ СИЛКАГЕЛІ

Роботу отримано 16 листопада 2001 р.

Затверджено до друку Вченою радою ІФКС НАН України

Рекомендовано до друку семінаром відділу теорії розчинів

Виготовлено при ІФКС НАН України

© Усі права застережені